LIF and IR Dip Spectra of Jet-Cooled *p*-Aminophenol−M (M = CO, N_2): Hydrogen-Bonded or Van der Waals-Bonded Structure?

Hirotoshi Mori,[†] Hitomi Kugisaki,[†] Yoshiya Inokuchi,[‡] Nobuyuki Nishi,[‡] Eisaku Miyoshi,[§] Kenji Sakota,[†] Kazuhiko Ohashi,[†] and Hiroshi Sekiya*[,†]

Department of Chemistry, Faculty of Sciences, and Graduate School of Molecular Chemistry, Faculty of Science, Kyushu University, 6-10-1 Hakozaki, Higashi-ku Fukuoka 812-8581, Japan, Institute for Molecular Science, Okazaki National Research Institutes, Myodaiji, Okazaki, 444-8585, Japan, and Graduate School of Engineering Sciences, Kyushu University, 6-1 Kasuga-Park, Fukuoka 816-8580, Japan

Received: December 18, 2001; In Final Form: March 12, 2002

Intermolecular interaction and stable structures of the *p*-aminophenol−M (M=CO, N_2) 1:1 complexes have been studied by measuring the $S_1 \leftarrow S_0$ ($\pi\pi^*$) fluorescence excitation spectra and the IR dip spectra in the OH and NH stretch region combined with ab initio calculations. The S_1-S_0 electronic origin of the CO complex is 141 cm^{-1} red shifted from the origin of the monomer. The red shift for the CO complex is smaller than 153 cm^{-1} for the N_2 complex, although the molecular polarizability of carbon monoxide is larger than that of molecular nitrogen. The OH stretching frequency of the CO complex is 26 cm^{-1} red shifted from that of the monomer in the IR dip spectrum, but the N_2 complex shows no shift. On the basis of these findings we conclude that carbon monoxide is bonded to the OH group via a hydrogen bond, whereas nitrogen is van der Waals-bonded to the π cloud of the aromatic ring.

1. Introduction

Recent progress in spectroscopic techniques has enabled us to obtain detailed information on the intermolecular hydrogen bond in the isolated state. The hydrogen-bonded complexes of an aromatic molecule with polar solvent molecules have been extensively studied with various spectroscopic methods combined with ab initio and density functional theory calculations. In particular, the IR dip spectroscopy is a very powerful tool to investigate the intermolecular hydrogen bond in isolated clusters and complexes.[1,2] The measurement of the OH, CH, and NH stretching frequencies provides direct information on the strength of the hydrogen bond. An aromatic molecule which has a hydroxyl or an amino group can form strong intermolecular hydrogen bond with polar molecules. Structures and intermolecular hydrogen bond in various clusters have been well characterized by IR dip spectroscopy.[1,2] But the characterization of a weak hydrogen bond is difficult as compared with the strong hydrogen bond, because of smaller changes in the vibrational frequencies.

Carbon monoxide and molecular nitrogen have isoelectronic structures and have similar polarizabilities to argon. These molecules form van der Waals complexes with benzene and halobenzenes.[3−7] In contrast, hydrogen-bonded structures have been observed in the complexes of phenol−CO and phenol−N_2.[8−10] The binding energies are determined to be 659 ± 20 and 435 ± 20 cm^{-1}, respectively, for the ground-state phenol−CO and phenol−N_2.[8] These energies are much smaller than a hydrogen-bonding energy of 1916 ± 30 cm^{-1} for the ground-state phenol−H_2O.[11] The OH stretching frequency of phenol−N_2 is significantly lower than that of phenol.[12] The decrease in the OH stretching frequency is consistent with the hydrogen-bonded structure proposed by Müller-Dethlefs and co-workers.[8−10] A similar intermolecular hydrogen bond is observed in resorcinol (1,3-hydroxybenzene)−CO.[13] The existence of a weak intermolecular hydrogen bond is also suggested in tropolone−CO_2.[14−16] These complexes have planar structures and the solvent molecule is located in the molecular plane of the aromatic or pseudoaromatic ring. In such planar complexes the interaction between the electric dipole moment of the OH or CO group of the chromophore and the electric quadrupole moment of the solvent molecule plays a crucial role to stabilize the complex.[8−10,12−14]

The carbon monoxide and nitrogen molecules may form an intermolecular hydrogen bond with the NH_2 group. The aniline−CO and aniline−N_2 complexes have been studied by electronic and IR dip spectroscopy.[17−20] The carbon monoxide or nitrogen molecules are considered to be bound to the π cloud of the aromatic ring by van der Waals interaction,[17,18] while the existence of a hydrogen-bonding interaction between carbon monoxide and the NH_2 group has been suggested by ab initio calculations.[19,20]

We have measured the electronic and IR dip spectra of the complexes of *p*-aminophenol (*p*AP) with carbon monoxide or nitrogen to investigate the effects of the substitution of the NH_2 group to the hydrogen atom at the para-position of phenol on the intermolecular interaction and stable structure. It has been found that carbon monoxide is bonded to the OH group, whereas nitrogen is bound on the aromatic ring, although both carbon monoxide and nitrogen are bonded to the OH group in phenol−CO, $-N_2$.[8,9] The difference in the geometry and intermolecular interaction between the two complexes are discussed on the basis of the observed vibrational frequencies, microscopic spectral shifts, and calculated stable structures.

* To whom correspondence should be addressed. E-mail: hsekiscc@mbox.nc.kyushu-u.ac.jp.

[†] Faculty of Sciences, and Graduate School of Molecular Chemistry, Faculty of Science, Kyushu University.

[‡] Institute for Molecular Science, Okazaki National Research Institute.

[§] Graduate School of Engineering Sciences, Kyushu University.

10.1021/jp014594j CCC: $22.00
Published on Web 04/25/2002

2. Experimental Section

The experimental apparatus for the measurement of the LIF spectrum was essentially the same as that reported previously.[21,22] The reagent *p*AP was purchased from Wako Pure Chemical Industries and was used without further purification. The *p*AP−M (M=CO, N_2) complexes were generated in a supersonic free jet expansion by heating *p*AP at ca. 130 °C. A reservoir containing the carbon monoxide or nitrogen gas was placed between a nozzle housing and a He carrier gas reservoir to control the concentration of carbon monoxide or nitrogen. The vaporized *p*AP was mixed with the solvent gas and He carrier gas and expanded into a vacuum chamber with a pulsed nozzle (General Valve, $D = 0.5$ mm). The backing pressure (P_0) was 2.0−3.0 atm. The *p*AP−M (M = CO, N_2) complexes were excited with an excimer laser pumped dye laser system (Lumonics EX-600 and HD-300). The output of the dye laser was frequency doubled in a KD*P crystal. The distance between the nozzle exit and a point where the laser beam crossing the molecular beam (X) was varied in the range of 1−3 cm. The LIF spectrum was measured by monitoring total fluorescence with a photomultiplier (Hamamatsu 1P28A). The electric current from the photomultiplier was fed into a digital oscilloscope (LeCroy 9310A) and the averaged signal was stored on a PC.

The IR dip spectrum was measured at Institute for Molecular Science. The UV radiation was generated by a Nd:YAG laser (Spectra Physics PRO-270) pumped OPO laser (Spectra Physics MOPO-730). The Nd:YAG laser was operated at 10 Hz. The IR laser was generated by a Nd:YAG laser (Continuum Powerlite 9010) pumped OPO laser (Continuum Mirage-3000). Both the IR and the UV lasers were coaxially introduced into a main vacuum chamber to cross the molecular beam. A typical delay time between the UV and IR lasers was 50 ns. The signals arising from ν_{UV} and $\nu_{UV} + \nu_{IR}$ were separately integrated and stored on a digital oscilloscope (LeCroy 9534A).

Ab initio calculations were carried out by using Gaussian98[23] and GAMESS[24] program packages with the MP2/cc-pVDZ level to obtain stable structures and binding energies for the *p*AP−M (M = CO, N_2) complexes and the natural populations[25] on the constituent atoms of *p*AP.

3. Results

LIF Spectra. Figure 1a shows the $S_1 \leftarrow S_0$ ($\pi\pi^*$) LIF spectrum of *p*AP in the electronic origin region. Figures 1b and 1c display the $S_1 \leftarrow S_0$ LIF spectra measured by introducing the carbon monoxide and nitrogen gas into the nozzle housing, respectively. The LIF spectrum of *p*AP is essentially the same as that reported previously.[21,26,27] The electronic origin bands of the *p*AP−CO and *p*AP−N_2 1:1 complexes are identified at 31249 and 31237 cm^{-1}, respectively. Only one species has been observed for both the *p*AP−CO and *p*AP−N_2 1:1 complexes. The frequencies of the in-plane bending mode of the aromatic ring ν_{6a} of the two complexes are identical to a value (444 cm^{-1}) of the monomer within the experimental errors. The red shifts in the $S \leftarrow S_0$ transition of the origin bands for the *p*AP−M (M = CO, N_2) complexes with respect to that for the *p*AP monomer are listed in Table 1. For comparison, we listed red shifts for phenol−CO and phenol−N_2,[8,10] and aniline−CO[28] and aniline−N_2[18] in Table 1. It is worth noting that the red shift for *p*AP−CO (141 cm^{-1}) is smaller than that (153 cm^{-1}) for *p*AP−N_2.

IR Dip Spectra of *p*AP−CO and *p*AP−N_2. Parts a−c of Figure 2 display the IR dip spectra of the *p*AP monomer, the CO complex, and the N_2 complex, respectively, obtained by exciting the electronic origin band of each species. The frequencies of the observed bands in the IR dip spectra are summarized in Table 2 together with the frequencies of *p*AP−H_2O.[21,27] The bands at 3405 and 3488 cm^{-1} in Figure 2a are assigned to the NH_2 symmetric (NH_{sym}) and NH_2 antisymmetric (NH_{asym}) stretch fundamentals of the monomer, respectively. The corresponding NH_{sym} and NH_{asym} stretch fundamentals of the CO complex are observed at 3403 and 3483 cm^{-1}, respectively. The band at 3660 cm^{-1} is assigned to the OH stretch fundamental. A prominent band at 3634 cm^{-1} in Figure 2b is assigned to the OH stretch fundamental of the *p*AP−CO

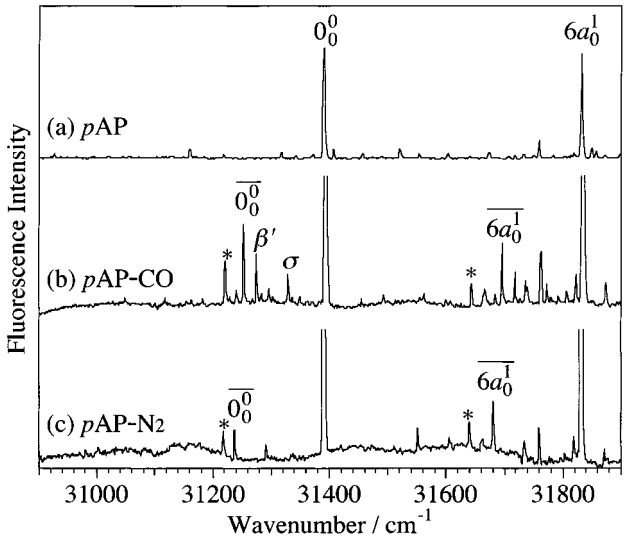

Figure 1. LIF spectra of *p*AP (a), *p*AP−CO (b), and *p*AP−N_2 (c). The asterisks in (b) and (c) denote the bands of the *p*AP−H_2O complex.[21] The bands at 22 and 76 cm^{-1} from the origin band of *p*AP−CO are assigned to intermolecular vibrations that are denoted by β' and σ. The assignment of the intermolecular vibrations has been made by analogy with the REMPI spectrum of phenol−CO.[8] The experimental conditions were $P_0 = 2.2$ atm and X/D = 40.

TABLE 1: Comparison of Spectral Redshifts of S_1-S_0 Transition Energy for *p*AP−M (M = Co, N_2)

	spectral red shift/cm^{-1}		
solvent (M)	*p*AP	phenol	aniline
CO	141	190[a]	351[a]
N_2	153	100[a]	129[a]
H_2O	172[c]	353[a]	

[a] Reference 2. [b] Reference 28. [c] Reference 21.

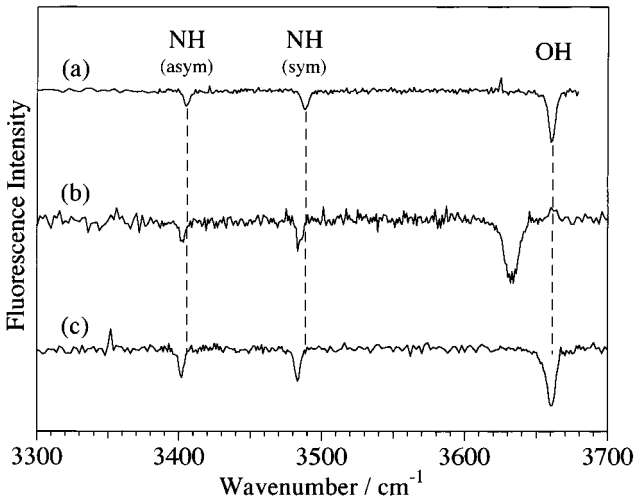

Figure 2. IR dip spectra of *p*AP monomer (a), *p*AP−CO (b), and *p*AP−N_2 (c). The experimental conditions were $P_0 = 2.0$ atm and X/D = 40.

TABLE 2: Vibrations in the IR Dip Spectra of *p*AP−M (M = CO, N_2)

	frequency/cm^{-1}[a]		
molecule	NH_{sym}	NH_{asym}	OH
*p*AP	3405	3488	3660
*p*AP−CO	3403 (2)	3483 (5)	3634 (26)
*p*AP−N_2	3402 (3)	3483 (5)	3660 (0)
*p*AP−H_2O[b]	3397 (8)	3479 (9)	3538 (122)

[a] The values in the parentheses indicate the red shifts from the corresponding monomer bands. [b] Reference 21.

TABLE 3: Calculated Structural Parameteres for *p*AP−M (M = CO, N_2)[a]

		*p*AP−CO		*p*AP−N_2	
bond length/Å	*p*AP	isomer A	isomer C	isomer A	isomer
R_{1-2}	0.967	0.968	0.969	0.988	0.968
R_{2-3}	1.376	1.373	1.371	1.403	1.373
R_{5-6}	1.019	1.020	1.020	1.034	1.020
R_{5-7}	1.019	1.020	1.020	1.033	1.020
R_{1-10}			2.320		
r[b]		3.2		3.0	

		*p*AP−CO		*p*AP−N_2	
bond angle/deg	*p*AP	isomer A	isomer C	isomer A	isomer
θ_{1-2-3}	106.8	107.1	107.5	110.2	107.1

		*p*AP−CO		*p*AP−N_2	
dihedral angle/deg [c]	*p*AP	isomer A	isomer C	isomer A	isomer
$\phi_{6-5-4-8}$	31.9	33.2	32.4	30.9	30.9

[a] Calculated at the MP2/cc-pVDZ level. [b] The distance between the center of aromatic ring and the center of mass of the solvent molecule. [c] The equilibrium inversion angle of the NH_2 group.

TABLE 4: Calculated Binding Energies for *p*AP−M (M = CO, N_2)

	binding energy/(kcal/mol)[a]			
complex	isomer A	isomer B	isomer C	isomer D
*p*AP−CO	2. 28	1.97	2.53	1.75
*p*AP−N_2	2.25	2.05	2.25	

[a] Calculated at the MP2/cc-pVDZ level. BSSE and ZPE corrected values.

complex. The OH stretch fundamental is 26 cm^{-1} red shifted due to the formation of the complex with CO. For the *p*AP−N_2 complex the OH stretch fundamental of *p*AP−N_2 is observed at 3660 cm^{-1}, while the NH_{sym} and NH_{asym} stretch fundamentals are observed at 3402 and 3483 cm^{-1}, respectively. It should be noted that the OH stretch frequency of *p*AP−N_2 shows no shift. This suggests that the OH group is free from the intermolecular hydrogen bond in the *p*AP−N_2 complex.

Calculated Structures for *p*AP−M (M = CO, N_2). Ab initio calculations at the level of MP2/cc-pVDZ were carried out to obtain stable structures and the binding energies for the *p*AP−CO and *p*AP−N_2 complexes. The structural parameters and the calculated binding energies are shown in Tables 3 and 4, respectively.

The optimized geometries of the *p*AP−CO complex are shown in Figure 3. Four structural isomers (A−D) have been obtained for the CO complex. In isomers A and B, the carbon monoxide molecule is bonded to the π electron cloud of the aromatic ring; the direction of carbon monoxide is different between isomers A and B. In isomers C and D, carbon monoxide is hydrogen bonded to the hydroxy proton. The carbon end of carbon monoxide is bonded to the hydroxy proton in isomer C, whereas the oxygen end is bonded to the hydroxy proton in isomer D. The distance between the carbon end and the hydroxy proton is calculated to be 2.30 Å for the most stable isomer C. The binding energy of isomer C is larger than that of isomer D by 0.78 kcal/mol.

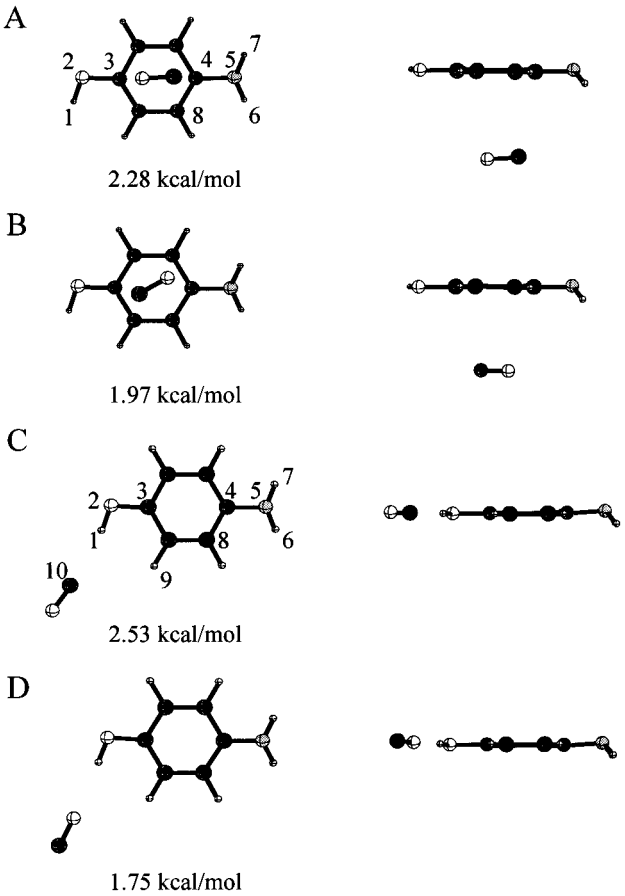

Figure 3. Fully optimized geometries of *p*AP−CO at the MP2/cc-pVDZ level. The structural parameters of isomers A and C are listed in Table 3.

The optimized geometries of the *p*AP−N_2 complex are shown in Figure 4. Three stable structures (A−C) are obtained for the *p*AP−N_2 complex. In isomers A and B, the N_2 molecule is bonded to the aromatic ring, while in isomer C, the N_2 molecule is bonded to the hydroxy proton. The binding energies of isomers A−C are very similar, and the binding energy of isomer A is identical to that of isomer C. This may suggest that the calculations at the level of MP2/cc-pVDZ are inadequate to estimate small differences in the binding energies among isomers A−C. Only a van der Waals-bonded structure has been observed; therefore, a possible candidate for the most stable structure is A or B.

4. Discussion

The most prominent result in this study is the observation of the large red shift (26 cm^{-1}) in the OH stretch fundamental for the *p*AP−CO 1:1 complex and no shift for the *p*AP−N_2 1:1 complex. The large red shift in the OH stretch fundamental for the *p*AP−CO complex is consistent with the most stable hydrogen-bonded structure predicted theoretically.[9] Isomers C and D of the *p*AP−CO complex in Figure 3 have planar hydrogen-bonded structures, where either the carbon end or the oxygen end of carbon monoxide is bonded to the hydroxy proton as shown in Figure 3. The carbon-end conformation may be preferable in the most stable structure as is the case for the phenol−CO complex.[9] In contrast, the observation of no shift

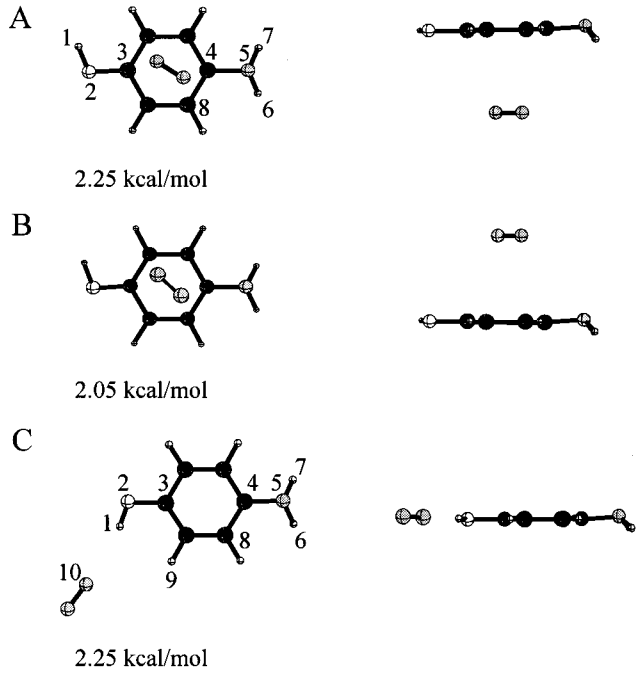

Figure 4. Fully optimized geometries of *p*AP−N_2 at the MP2/cc-pVDZ level. The structural parameters of isomers A and C are listed in Table 3.

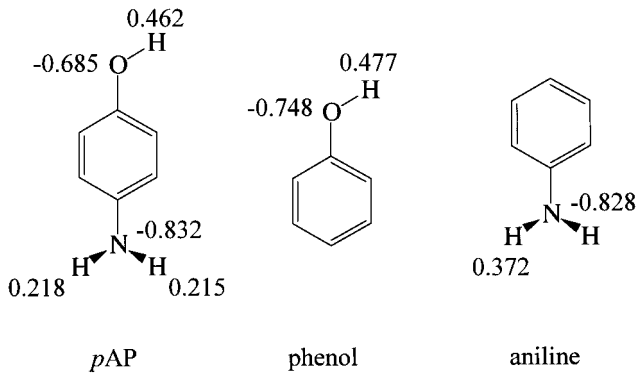

Figure 5. Natural charge on each atom of *p*AP, phenol, and aniline at the MP2/cc-pVDZ level.

in the OH stretch fundamental for *p*AP−N_2 indicates that the nitrogen molecule is not bonded to the OH group but to the π cloud of the aromatic ring. The strengths of the hydrogen-bonding interaction and the van der Waals interaction may determine the most stable structures of the *p*AP−CO and *p*AP−N_2 complexes.

In our previous study on the hydrogen-bonding interaction in the *p*-aminobenzonitrile−H_2O complex, we explained the change in the role of the amino group from a proton acceptor to a proton donor in terms with the atomic charges on the constituent atoms obtained by natural population analysis.[29] The substitution of the CN group decreases the negative charge on the amino nitrogen, whereas the positive charge on the amino proton increases, resulting in a stronger hydrogen bond between the amino proton and the oxygen atom of water than a hydrogen bond between the amino nitrogen and a hydrogen atom of water. By analogy, the charge density on the proton of the OH group must be important for the hydrogen-bonding interaction.

The calculated atomic charges in Figure 5 provide insights into the intermolecular interaction between the amino group and the solvent molecule. The NH_{sym} and NH_{asym} stretch frequencies of aniline−CO are 6.3 and 10.6 cm^{-1} lower than those of aniline. These shifts are significant, implying that the hydrogen-bonding interaction between the amino proton and carbon monoxide is responsible for stabilizing the complex. Recent theoretical calculations showed that carbon monoxide interacts with both the aromatic ring and the amino group in the most stable conformation.[19] Natural population analysis shows that the substitution of the OH group to aniline significantly decreases the atomic charge on the amino proton; therefore, the hydrogen-bonding interaction is insignificant and the van der Waals interaction is dominant in isomers A and B of *p*AP−CO. As a result, the hydrogen-bonded structure is more stable than the van der Waals structure in *p*AP−CO.

The above considerations about the intermolecular interaction in *p*AP−CO can be applied to elucidate the observation of van der Waals-bonded structure for *p*AP−N_2. The substitution of the amino group to the hydrogen atom at the para-position of phenol may decrease the hydrogen-bonding interaction between the hydroxy proton and nitrogen, but increase the van der Waals interaction due to the dipole−induced dipole interaction originating from a large dipole moment of the amino group in addition to the dispersive interaction.

The NH_{sym} and NH_{asym} stretch frequencies of *p*AP−N_2 are smaller than those of the monomer by 3 and 5 cm^{-1}, respectively. These shifts are similar to the corresponding shifts in the NH_{sym} and NH_{asym} stretch frequencies, 2.0 and 3.5 cm^{-1}, for aniline−N_2.[18] Such small red shifts in the NH_{sym} and NH_{asym} stretch frequencies may be due to nonlocal character of the NH_2 vibration. The motion of the NH_2 group involves the coordinates of the heavy atoms in the aromatic ring;[21,30] therefore, the NH_{sym} and NH_{asym} stretch frequencies slightly change even when the solvent molecule is not directly bonded to the amino group.

5. Conclusion

The frequency shifts in the OH stretch vibration clearly showed that the carbon monoxide molecule is hydrogen-bonded to the hydroxy proton of *p*AP in the *p*AP−CO complex, whereas the nitrogen molecule is bonded to the π cloud of the aromatic ring in the *p*AP−N_2 complex. It has been demonstrated that the substitution of the amino group to the hydrogen atom at the para-position of phenol easily switches the most stable conformation of the N_2 complex from the hydrogen-bonded structure to the van der Waals-bonded structure.

Acknowledgment. This work was supported in part by a Grant-in-Aid for Scientific Research No.1440177 from the Ministry of Education, Science, Sports and Culture.

References and Notes

(1) Ebata, T.; Fujii, A.; Mikami, N. *Int. Rev. Phys. Chem.* **1998**, *17*, 331.
(2) Dessent, C. E. H.; Müller-Dethlefs, K. *Chem. Rev.* **2000**, *100*, 3999.
(3) Sun, S.; Bernstein, E. R. *J. Phys. Chem.* **1996**, *100*, 13348.
(4) Brupbacher, T.; Bauder, A. *J. Chem. Phys.* **1993**, *99*, 9394.
(5) Weber, T.; Smith, A. M.; Riedle, E.; Neusser, H. J.; Schlag, E. W. *Chem. Phys. Lett.* **1990**, *175*, 79.
(6) Nathaniel, P. R.; Zwier, T. S. *Science* **1994**, *265*, 75.
(7) Tanabe, S.; Ebata, T.; Fujii, A.; Mikami, N. *Chem. Phys. Lett.* **1993**, *215*, 347.
(8) Heines, S. R.; Dessent, C. E. H.; Müller-Dethlefs, K. *J. Chem. Phys.* **1999**, *111*, 1947.
(9) Chapman, D. M.; Peel, J. B.; Müller-Dethlefs, K. *J. Chem. Phys.* **1999**, *111*, 1955.
(10) Ford, M. S.; Haines, S. R.; Pugliesi, I.; Dessent, C. E. H.; Müller-Dethlefs, K. *J. Electron. Spectrosc. Relat. Phenom.* **2000**, *112*, 231.
(11) Brauna, J. E.; Mehnerta, T.; Neusser, H. J. *Int. J. Mass Spectrosc.* **2000**, *203*, 1.
(12) Fujii, A.; Miyazaki, M.; Ebata, T.; Mikami, N. *J. Chem. Phys.* **1999**, *110*, 11125.

(13) Geppert, W. D.; Dessemt, C. E. H.; Müller-Dethlefs, K. *J. Phys. Chem. A* **1999**, *103*, 9687.

(14) MacKenzie, V. J.; Steer, R. P. *Res. Chem. Intermed.* **1998**, *24*, 803.

(15) MacKenzie, V. J.; Zgierski, M. Z.; Steer, R. P. *J. Phys. Chem. A* **1999**, *103*, 8389.

(16) Iwahashi, K.; Yamamoto, N.; Fukuchi, T.; Furusawa, J.; Sekiya, H. *Chem. Phys.* **2001**, *270*, 333.

(17) Yamanouchi, K.; Isogai, S.; Tsuchiya, S. *J. Mol. Struct.* **1986**, *146*, 394.

(18) Schmid, R. P.; Chowdhury, P. K.; Miyawaki, J.; Ito, F.; Sugawara, K.; Nakanaga, T.; Takeo, H.; Jones, H. *Chem. Phys*. **1997**, *218*, 291.

(19) Ikeshoji, T.; Nakanaga, T. *J. Mol. Struct. (THEOCHEM)* **1999**, *489*, 47.

(20) Kugisaki, H.; Sakota, K.; Yamamoto, N.; Ohashi, K.; Sekiya, H. Unpublished.

(21) Mori, H.; Kugisaki, H.; Inokuchi, Y.; Nishi, N.; Miyoshi, E.; Sakota, K.; Ohashi, K.; Sekiya, H. *Chem. Phys.* **2002**, *277*, 105.

(22) Nishi, K.; Sekiya, H.; Kawakami, H.; Mori, A.; Nishimura, Y. *J. Chem. Phys.* **1998**, *109*, 1589.

(23) Frisch, M. J.; Trucks, G. W.; Schlegel, H. B.; Scuseria, G. E.; Robb, M. A.; Cheeseman, J. R.; Zakrzewski, V. G.; Montgomery, J. A.; Stratmann, R. E.; Burant, J. C.; Dapprich, S.; Millam, J. M.; Daniels, A. D.; Kudin, K. N.; Strain, M. C.; Farkas, O.; Tomasi, J.; Barone, V.; Cossi, M.; Cammi, R.; Mennucci, B.; Pomelli, C.; Adamo, C.; Clifford, S.; Ochterski, J.; Petersson, G. A.; Ayala, P. Y.; Cui, Q.; Morokuma, K.; Malick, D. K.; Rabuck, A. D.; Raghavachari, K.; Foresman, J. B.; Cioslowski, J.; Ortiz, J. V.; Baboul, A. G.; Stefanov, B. B.; Liu, G.; Liashenko, A.; Piskorz, P.; Komaromi, I.; Gomperts, R.; Martin, R. L.; Fox, D. J.; Keith, T.; Al-Laham, M. A.; Peng, C. Y.; Nanayakkara, A.; Gonzalez, C.; Challacombe, M.; Gill, P. M. W.; Johnson, B.; Chen, W.; Wong, M. W.; Andres, J. L.; Gonzalez, C.; Head-Gordon, M.; Replogle, E. S.; Pople, J. A. *Gaussian 98*, Revision A.7; Gaussian, Inc.; Pittsburgh, PA, 1998.

(24) Schmidt, M. W.; Baldridge, K. K.; Boatz, J. A.; Elbert, S. T.; Gordon, M. S.; Jensen, J. H.; Koseki, S.; Matsunaga, N.; Nguyen, K. A.; Su, S. J.; Windus, T. L.; Dupuis, M.; Montgomery, J. A. *J. Comput. Chem.* **1993**, *14*, 1347.

(25) Reed, A. E.; Curtiss, L. A.; Weinhold, F. *Chem. Rev.* **1988**, *88*, 899.

(26) Wategaonkar, S.; Doraiswamy, S. *J. Chem. Phys.* **1996**, *105*, 1786.

(27) Gerhards, M.; Unterberg, C. *Appl. Phys. A* **2001**, *72*, 273.

(28) Jackel, J. G.; Jones, H. *Chem. Phys.* **1999**, *247*, 321.

(29) Sakota, K.; Yamamoto, N.; Ohashi, K.; Sekiya, H.; Saeki, M.; Ishiuchi, S.; Sakai, M.; Fujii, M. *Chem. Phys. Lett.* **2001**, *341*, 70.

(30) Becucci, M.; Castellucci, E.; López-Tocón, I.; Pietraperzia, G.; Salvi, P. R.; Caminati, W. *J. Phys. Chem. A* **1999**, *103*, 8946.